

## Lecture 6. Monin-Obukhov similarity theory (Garratt 3.3)

*In this lecture...*

- Similarity theory for wind and scalar profiles in stratified surface layers.
- Stability correction to bulk surface-air transfer coefficients.

*Stability correction to vertical profiles in the surface layer*

Because so many BL measurements are made within the surface layer (i. e. where wind veering with height is insignificant) but stratification effects can be important at standard measurement heights of 2 m (for temperature and moisture) and 10 m (for winds), it is desirable to correct the log-layer profiles for stratification effects.

Based on the scaling arguments of last lecture, Monin and Obukhov (1954) suggested that the vertical variation of mean flow and turbulence characteristics in the surface layer should depend only on the surface momentum flux as measured by friction velocity  $u_*$ , buoyancy flux  $B_0$ , and height  $z$ . One can form a single nondimensional combination of these, which is traditionally chosen as the **stability parameter**

$$\zeta = z/L. \quad L = -u_*^3 / \kappa B_0 \quad (6.1)$$

The logarithmic scaling regime of last time corresponds to  $\zeta \ll 1$ .

Thus, within the surface layer, we must have

$$(kz/u_*)(du/dz) = \Phi_m(\zeta) \quad (6.2)$$

$$-(kz/\theta_*)(d\theta/dz) = \Phi_h(\zeta) \quad (6.3)$$

where  $\Phi_m(\zeta)$  and  $\Phi_h(\zeta)$  are nondimensional **stability functions** which relate the fluxes of momentum and  $\theta$  (i. e. sensible heat) to their mean gradients. Other adiabatically conserved scalars should behave similarly to  $\theta$  since the transport is associated with eddies which are too large to be affected by molecular diffusion or viscosity. To agree with the log layer scaling,  $\Phi_m(\zeta)$  and  $\Phi_h(\zeta)$  should approach 1 for small  $\zeta$ .

We can express (6.2) and (6.3) in other equivalent forms. First, we can regard them as defining surface layer eddy viscosities:

$$K_m = \overline{-u'w'_0} / (du/dz) = u_*^2 / (\Phi_m(\zeta)u_*/kz) = kzu_*/\Phi_m(\zeta) \quad (6.4)$$

$$K_h = \overline{-w'\theta'_0} / (d\theta/dz) = u_*\theta_*/(\Phi_h(\zeta)\theta_*/kz) = kzu_*/\Phi_h(\zeta) \quad (6.5)$$

By analogy to the molecular Prandtl number, the turbulent Prandtl number is their ratio:

$$\text{Pr}_t = K_m/K_h = \Phi_h(\zeta) / \Phi_m(\zeta). \quad (6.6)$$

Another commonly used form of the stability functions is to measure stability with gradient Richardson number  $\text{Ri}$  instead of  $z$ . Recalling that  $N^2 = -db/dz$ , and again noting that the surface layer is thin, so vertical fluxes do not vary significantly with height within it,  $\text{Ri}$  is related to  $z$  as follows:

$$\text{Ri} = (-db/dz) / (du/dz)^2$$

$$\begin{aligned}
&= (\overline{w'b'_0}/K_h) / (-\overline{u'w'_0}/K_m)^2 \\
&= (B_0 \Phi_h(\zeta) / kz u_*) / (u_*^2 \Phi_m(\zeta) / kz u_*)^2 \\
&= \zeta \Phi_h / \Phi_m^2.
\end{aligned} \tag{6.7}$$

Given expressions for  $\Phi_m(\zeta)$  and  $\Phi_h(\zeta)$ , we can write  $\zeta$  and hence the stability functions and eddy diffusivities in terms of Ri. The corresponding formulas for dependence of eddy diffusivity on Ri are often used by modellers even outside the surface layer, with the neutral  $K_m$  and  $K_h$  estimated as the product of an appropriate velocity scale and lengthscale.

### Field Experiments

The stability functions must be determined empirically. In the 1950-60s, several field experiments were conducted for this purpose over regions of flat, homogeneous ground with low, homogeneous roughness elements, culminating in the 1968 Kansas experiment. This used a 32 m instrumented tower in the middle of a 1 mi<sup>2</sup> field of wheat stubble. Businger et al. (1971, *JAS*, **28**, 181-189) documented the relations below, which are still accepted:

$$\Phi_m = \begin{cases} (1 - \gamma_1 \zeta)^{-1/4}, & \text{for } -2 < \zeta < 0 \text{ (unstable)} \\ 1 + \beta \zeta, & \text{for } 0 \leq \zeta < 1 \text{ (stable)} \end{cases} \tag{6.8}$$

$$\Phi_h = \begin{cases} \text{Pr}_{tN} (1 - \gamma_2 \zeta)^{-1/2}, & \text{for } -2 < \zeta < 0 \text{ (unstable)} \\ \text{Pr}_{tN} + \beta \zeta, & \text{for } 0 \leq \zeta < 1 \text{ (stable)} \end{cases} \tag{6.9}$$

The values of the constants determined by the Kansas experiment were

$$\text{Pr}_{tN} = 0.74, \quad \beta = 4.7, \quad \gamma_1 = 15, \quad \gamma_2 = 9.$$

The quality of the fits to observations are shown on the next page. Other experiments have yielded somewhat different values of the constants (Garratt, Appendix 4, Table A5), so we will follow Garratt (p. 52) and Dyer (1974, *Bound-Layer Meteor.*, **7**, 363-372) and assume:

$$\text{Pr}_{tN} = 1, \quad \beta = 5, \quad \gamma_1 = \gamma_2 = 16. \tag{6.10}$$

In neutral or stable stratification, this implies  $\Phi_m = \Phi_h$ , i. e. pressure perturbations do not affect the eddy transport of momentum relative to scalars such as heat, and the turbulent Prandtl number is 1. In unstable stratification, the eddy diffusivity for scalars is more than for momentum.

Solving these relations for Ri,

$$\zeta = \begin{cases} \text{Ri}, & \text{for } -2 < \text{Ri} < 0 \text{ (unstable)} \\ \frac{\text{Ri}}{1-5\text{Ri}}, & \text{for } 0 < \text{Ri} < 0.2 \text{ (stable)} \end{cases} \tag{6.11}$$

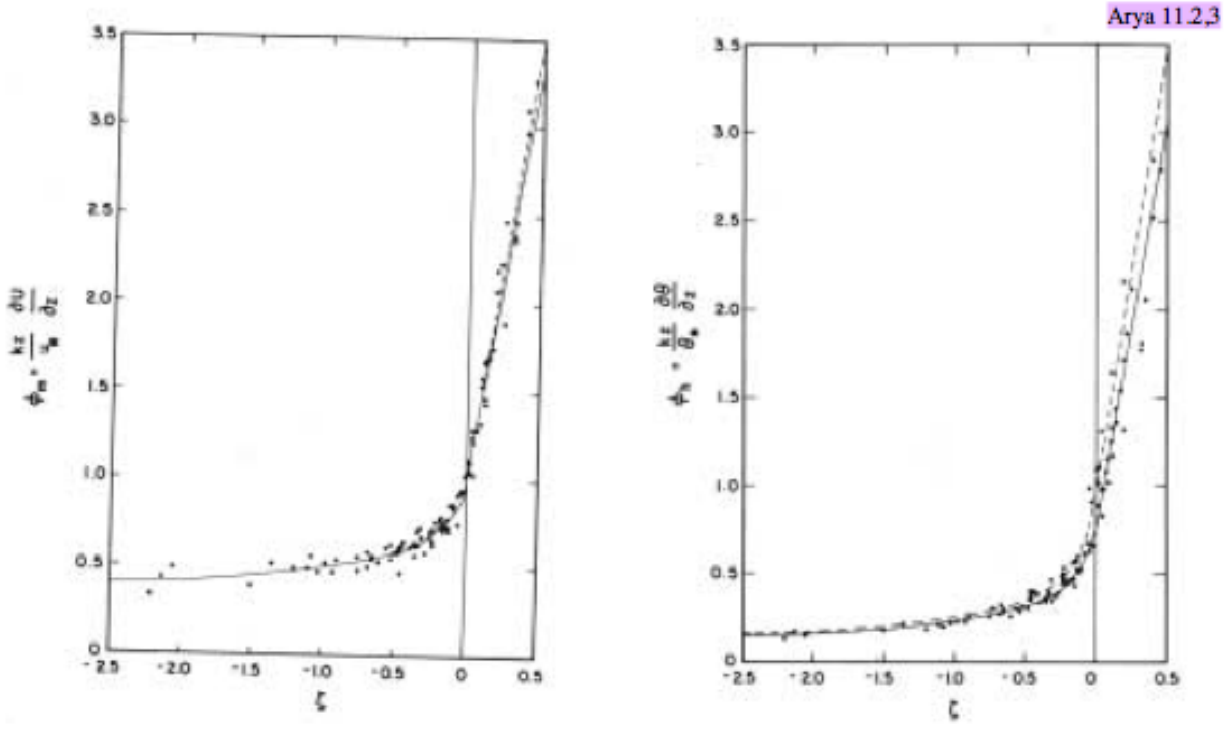


Fig. 6.1: Empirical determination of stability functions from Kansas experiment.

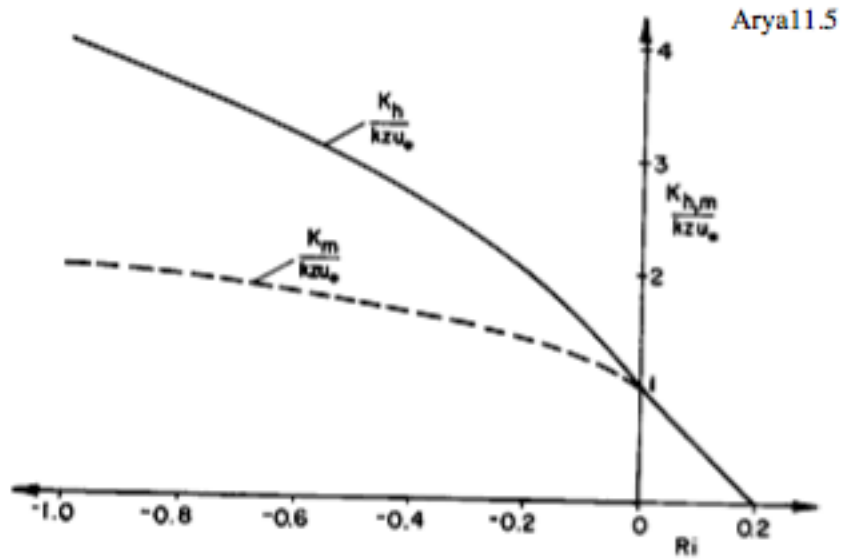


Fig. 6.2: Nondimensional eddy viscosity  $\Phi_m^{-1}$  and diffusivity  $\Phi_h^{-1}$  as functions of stability, measured by Ri.

*Limiting cases* (Garratt, p. 50)

- (i) *Neutral limit*:  $\Phi_m, \Phi_h \rightarrow 1$  as  $\zeta \rightarrow 0$  as expected, recovering log-layer scaling for  $z \ll |L|$ .
- (ii) *Stable limit*: Expect eddy size to depend on  $L$  rather than  $z$  ( **$z$ -less scaling**), since our scaling analysis of last time suggests that stable buoyancy forces tend to suppress eddies with a scale larger than  $L$ . This implies that the eddy diffusivity

$$\begin{aligned} K_m &= kz u^* / \Phi_m \propto (\text{length}) (\text{velocity}) = Lu^* \\ \Rightarrow \Phi_m &\propto z/L = \zeta \quad \text{as } \zeta \rightarrow +\infty \end{aligned} \quad (6.12)$$

and similarly for  $K_h$ . The empirical formulas imply  $\Phi_m \sim \beta \zeta$  for large  $\zeta$ , which is consistent with this limit.

- (iii) *Unstable limit*. Convection replaces shear as the main source of eddy energy, so we expect the eddy velocity to scale with the buoyancy flux  $B_0$  and not the friction velocity. We still assume that the size of the eddies that carry most of the vertical fluxes is limited by the distance  $z$  to the boundary. In this '**free convective scaling**', the eddy velocity scale is  $u_f = (B_0 z)^{1/3}$  and the eddy viscosity should go as

$$\begin{aligned} K_m &= kz u^* / \Phi_m \propto (\text{length}) (\text{velocity}) = zu_f \\ \Rightarrow \Phi_m &\propto u^* / u_f \propto (-z/L)^{-1/3} = (-\zeta)^{-1/3} \quad \text{as } \zeta \rightarrow -\infty \end{aligned} \quad (6.13)$$

A similar argument applies for the scalar stability function  $\Phi_h$ . The empirical relations go as  $(-\zeta)^{-1/2}$  for scalars and  $(-\zeta)^{-1/4}$  for momenta, which are close but not identical to  $(-\zeta)^{-1/3}$ . Note reliable measurements only extend out to  $\zeta = -2$ , so free convective scaling may be physically realized at larger  $|\zeta|$ .

*Wind and thermodynamic profiles*

The similarity relations can be integrated with respect to height to get:

$$u(z) = \frac{u_*}{k} \left[ \log \left( \frac{z}{z_0} \right) - \Psi_m(\zeta) \right], \quad (6.14)$$

$$\theta(z) = \theta_0 - \frac{\theta_*}{k} \left[ \log \left( \frac{z}{z_T} \right) - \Psi_h(\zeta) \right], \quad (6.15)$$

(and similarly for other scalars), where if  $x = (1 - \gamma_1 \zeta)^{1/4}$ ,

$$\begin{aligned} \Psi_m(\zeta) &= \int_0^\zeta [1 - \Phi_m(\zeta')] d\zeta' / \zeta' \\ &= \begin{cases} \log \left[ \left( \frac{1+x^2}{2} \right) \left( \frac{1+x}{2} \right)^2 \right] - 2 \tan^{-1} x + \frac{\pi}{2}, & \text{for } -2 < \zeta < 0 \text{ (unstable)} \\ -\beta \zeta, & \text{for } 0 \leq \zeta \text{ (stable)} \end{cases} \end{aligned} \quad (6.16)$$

$$\Psi_h(\zeta) = \int_0^\zeta [1 - \Phi_h(\zeta')] d\zeta' / \zeta'$$

$$= \begin{cases} 2 \log\left(\frac{1+x^2}{2}\right), & \text{for } -2 < \zeta < 0 \text{ (unstable)} \\ -\beta\zeta. & \text{for } 0 \leq \zeta \text{ (stable)} \end{cases} \quad (6.17)$$

Wind profiles in stable, neutral, and unstable conditions are shown in the figure below. Low-level wind and shear are reduced compared to the log profile in unstable conditions, for which  $K_m$  is larger.

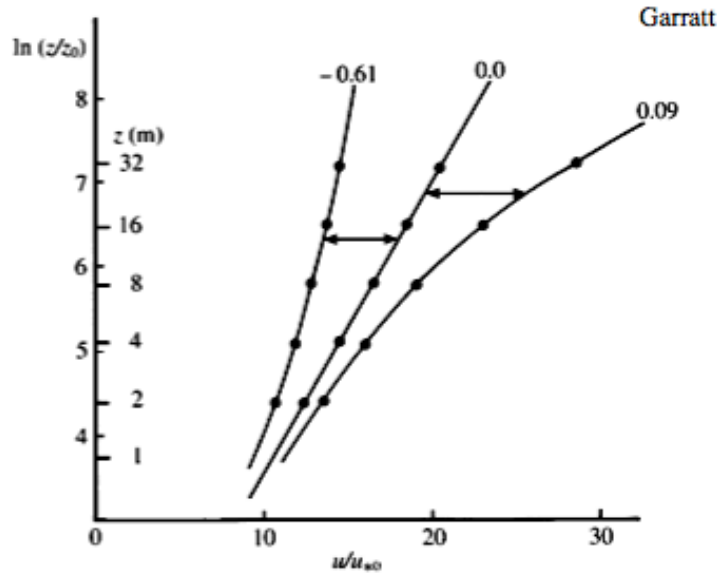


**Fig.3.5** Three wind profiles from the Kansas field data (Izumi, 1971) plotted in normalized form at three values of the gradient  $Ri$  ( $z = 5.66$  m). Both normalized and absolute heights are shown, whilst the magnitude of the horizontal arrows indicates the effect of buoyancy on the wind relative to the neutral profile (see Eq. 3.34).

From (6.14) and (6.15), we derive bulk aerodynamic coefficients for non-neutral conditions:

$$C_D = \frac{k^2}{[\log(z_R / z_0) - \Psi_m(z_R / L)]^2}, \quad (6.18)$$

$$C_H = \frac{k^2}{[\log(z_R / z_0) - \Psi_m(z_R / L)][\log(z_R / z_T) - \Psi_h(z_R / L)]} \quad (6.19)$$

These decrease considerably in stable conditions (see figure on next page).

The main use of these transfer coefficients is to compute the surface fluxes from the wind and thermodynamic quantities measured or computed at a reference level  $z_R$ . For a numerical model,  $z_R$  is the lowest grid level for horizontal winds and scalars. In either case, this approach is only valid if  $z_R$  is in the surface layer; this condition can easily be violated for strongly stable boundary layers for the coarse vertical grid of many large-scale numerical models.

Garratt

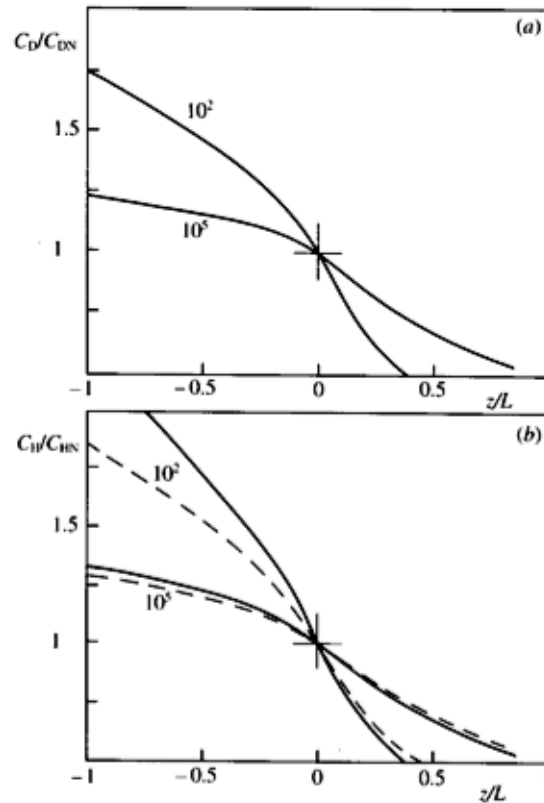


Fig. 3.7 Values of (a)  $C_D/C_{DN}$  and (b)  $C_H/C_{HN}$  as functions of  $z/L$  for two values of  $z/z_0$  as indicated. In (b), the solid curves have  $z_0 = z_T$ , and the pecked curves have  $z_0/z_T = 7.4$  (see Chapter 4).

A practical complication is that  $L$  depends on the surface momentum and buoyancy fluxes, which are what we are trying to compute. Thus, we must solve (6.18) and (6.19) simultaneously with the definition of the Obukhov length,

$$L = -u_*^3/kB_0 \tag{6.20}$$

To compute  $L$  from reference-level quantities, we note that by definition of  $C_D$ ,

$$u_*^2 = C_D u^2(z_R) \tag{6.21}$$

Although not precisely correct, it is generally a good approximation to assume  $C_H$  can also be applied to virtual temperature  $\theta_v$  as well as  $\theta$ , so that the surface buoyancy flux can be computed

$$B_0 = C_H u(z_R) \frac{g}{\theta_{v0}} [\theta_{v0} - \theta_v(z_R)] \tag{6.22}$$

Substituting these formulas for  $u_*$  and  $B_0$  into (6.20), we have expressed  $L$  in terms of reference level quantities together with  $C_D$  and  $C_H$ .

We must now solve the three simultaneous nonlinear equations (6.18), (6.19) and (6.20) for  $C_D$ ,  $C_H$  and  $L$ . One approach for doing this is iterative and relies on the fact that the stability dependence of  $C_D$ ,  $C_H$  is not too strong. Starting with an estimate of  $L$ , we solve for  $C_D$ ,  $C_H$ . Using these coefficients, we infer  $u_*$  and  $B_0$  and thereby get a new estimate of  $L$ . The iteration is repeated until it converges (which it generally does). We can start the iteration by assuming

neutral conditions ( $L = \infty$ ). The problem is further complicated over the ocean, where  $z_0$  and  $z_T$  depend on  $u_*$ . A popular simplification is to use a computationally efficient approximation to the iterative solution, e.g. Louis 1979, *Bound. Layer Meteor.*, **17**, 187-202.

*Scaling for the entire boundary layer- the turbulent Ekman layer* (Garratt, 3.2)

In general, the BL depth  $h$  and turbulence profile depend on many factors, including history, stability, baroclinicity, clouds, presence of a capping inversion, etc. Hence universal formulas for the velocity and thermodynamic profiles above the surface layer (i. e. where transports are primarily by the large, BL-filling eddies) are rarely applicable.

However, a couple of special cases are illuminating to consider. The first is a well-mixed BL (homework), in which the fluxes adjust to ensure that the tendency of  $\theta$ ,  $q$ , and velocity remain the same at all levels. Well mixed BLs are usually either strongly convective, or strongly driven stable BLs capped by a strong inversion. As will be further discussed in later lectures, mixed layer models incorporating an entrainment closure for determining the rate at which BL turbulence incorporates above-BL air into the mixed layer are widely used.

The other interesting (though rarely observable) case is a steady-state, neutral, barotropic BL. This is the turbulent analogue to a laminar Ekman layer. Here, the fundamental scaling parameters are  $G = \mathbf{u}_g$ ,  $f$ , and  $z_0$ . Out of these one can form one independent nondimensional parameter, the surface Rossby number  $Ro_s = G/fz_0$  (which is typically  $10^4 - 10^8$ ). The friction velocity (which measures surface stress) must have the form

$$u_*/G = F(Ro_s) \quad (6.23)$$

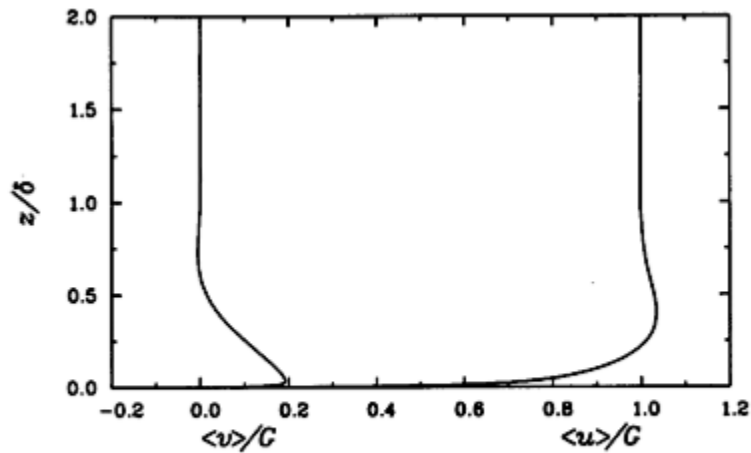
Hence, one can also regard  $u_*/G$  (which has a typical value of 0.01-0.1) as a proxy nondimensional control parameter in place of  $Ro_s$ . The steady-state BL momentum equations are

$$f(u - u_g) = -\frac{d}{dz} \overline{v'w'}, \quad (6.24)$$

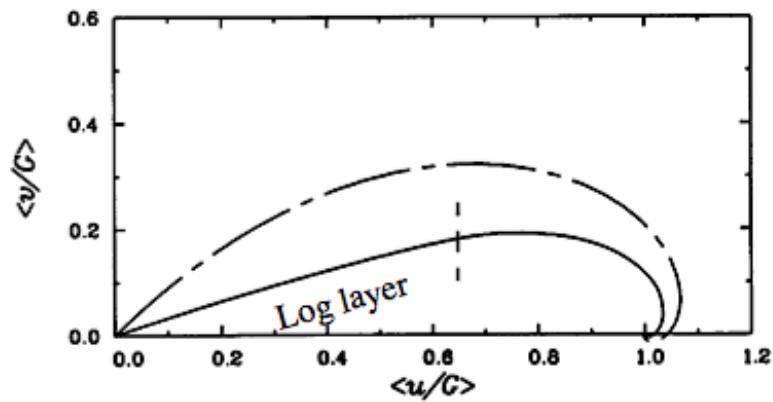
$$f(v - v_g) = \frac{d}{dz} \overline{u'w'}. \quad (6.25)$$

On the next page are velocity and momentum flux profiles from a direct numerical simulation (384×384×85 gridpoints) in which  $u_*/G = 0.053$  (Coleman 1999, *J. Atmos. Sci.*, **56**, 891-900). The geostrophic wind is oriented in the  $x$  direction, and is independent of height (the barotropic assumption). Height is nondimensionalized by  $\delta = u_*/f$ . In the thin surface layer, extending up to  $z = 0.02\delta$ , the wind increases logarithmically with height without appreciable turning (this is most clearly seen on the wind hodograph), and is turned at  $20^\circ$  from geostrophic (this angle is an increasing function of  $u_*/G$ ). The neutral BL depth, defined as the top of the region of significantly ageostrophic mean wind, is

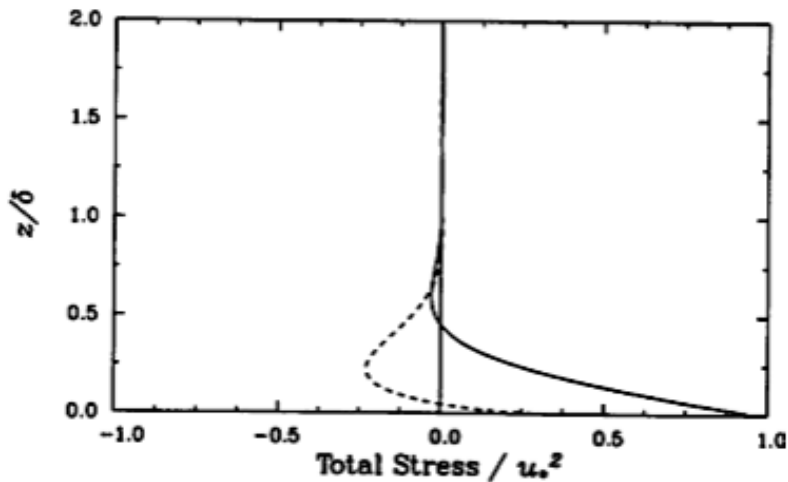
$$h_N = 0.8u_*/f. \quad (6.26)$$



Wind profiles in a neutral barotropic BL with  $u_*/G = 0.053$  (Coleman 1999).



Wind hodograph (dashed = Ekman layer). Log (surface) layer is part of profile to right of dashes.



Stress profiles in geostrophic coordinate system. Solid = in direction of  $\mathbf{u}_g$ , dashed = transverse dir.

Fig. 6.5: Wind and stress profiles in a numerically simulated turbulent barotropic Ekman layer



For  $u_* = 0.3 \text{ m s}^{-1}$  and  $f = 10^{-4} \text{ s}^{-1}$ ,  $H_N = 2.4 \text{ km}$ . Real ABLs are rarely this deep because of stratification aloft, but fair approximations to the idealized turbulent Ekman layer can occur in strong winds over the midlatitude oceans. The wind profile qualitatively resembles an Ekman layer with a thickness  $0.12u_*/f$ , except much more of the wind shear is compressed into the surface layer.

The profiles of ageostrophic wind and momentum flux depend only very weakly on  $Ro_s$  above the surface layer. Below we show a scaling using  $u_*$  and  $f$  that collapses these into universal profiles. These wind and stress profiles can be matched onto a  $z_0$ -dependent surface log-layer; the matching height (i. e. the top of the surface layer) and the implied surface wind turning angle depend upon  $z_0$ ; in this way the profiles can apply to arbitrary  $Ro_s$ .

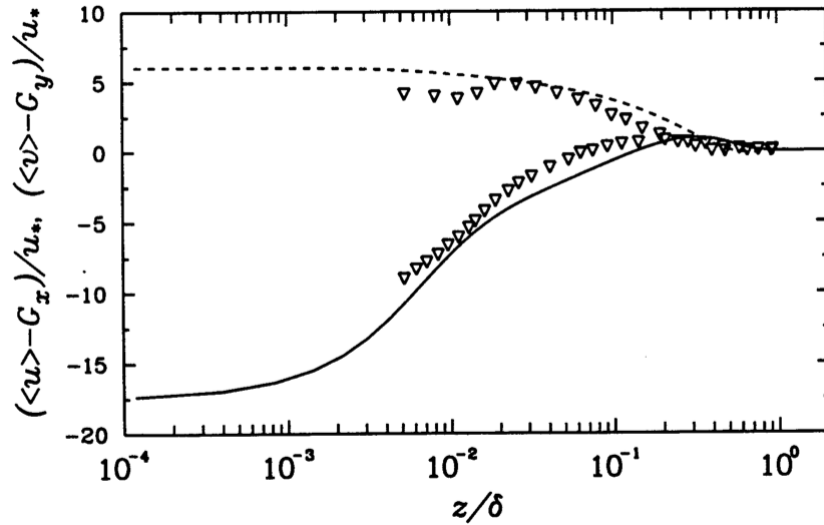


Fig. 6.6: Scaled ageostrophic wind (solid: LES; triangles: lab expt.) for a turbulent Ekman layer. A log-profile in the surface layer ( $z/\delta < 0.02$ ) matches onto universal profiles above.

As we go up through the boundary layer, the magnitude of the momentum flux will decrease from  $u_*^2$  in the surface layer to near zero at the BL top, so throughout the BL, the momentum flux will be  $O(u_*^2)$ , and the turbulent velocity perturbations  $u'$ ,  $w'$  should scale with  $u_*$  to be consistent with this momentum flux). We assume that the BL depth scales with  $\delta = u_*/f$ . These scalings suggest a nondimensionalization of the steady state BL momentum equations (6.24) and (6.25):

$$\frac{u - u_g}{u_*} = -\frac{d(\overline{v'w'}/u_*^2)}{d(z/\delta)} \quad (6.27)$$

$$\frac{v - v_g}{u_*} = \frac{d(\overline{u'w'}/u_*^2)}{d(z/\delta)} \quad (6.28)$$

If we adopt a coordinate system in which the  $x$  axis is in the direction of the surface-layer wind, the boundary conditions on the momentum flux are

$$\overline{u'w'}/u_*^2 \rightarrow 1 \text{ and } \overline{v'w'}/u_*^2 \rightarrow 0 \text{ as } z/\delta \rightarrow 0 \text{ (i. e. at surface layer top)} \quad (6.29)$$

$$\overline{u'w'}/u_*^2 \rightarrow 0 \text{ and } \overline{v'w'}/u_*^2 \rightarrow 0 \text{ as } z/\delta \rightarrow \infty \quad (6.30)$$

If we assume that the momentum flux depends only on wind shear and height, this is consistent with universal **velocity defect laws**:

$$\frac{u - u_g}{u_*} = F_x(z/\delta), \quad \frac{v - v_g}{u_*} = F_y(z/\delta) . \quad (6.31)$$

and similarly for momentum flux scaled with  $u_*^2$ . These universal profiles can then be deduced from either lab experiments or numerical simulations of turbulent Ekman layers. . The figure below shows that Coleman's simulations and laboratory experiments with different parameters are consistent with the same  $F_x$  and  $F_y$ , supporting their universality. One can see that at  $h_N = 0.8\delta$ , the velocity defects are very close to zero (geostrophic flow), while at  $z \approx 0.02\delta$ , the  $v$  defect has flattened out with  $F_y(0) \approx 5$ . This corresponds to the top of the surface layer.

In the surface layer, these universal functions cease to apply and the logarithmic wind profile  $u(z) = (u_*/k) \ln(z/z_0)$ ,  $v(z) = 0$  must match onto the defect laws. In particular, this means that  $F_y(0) = -v_g/u_*$ , i. e. that  $v_g \approx -5u_*$ . From the overall geostrophic wind magnitude  $G$ , we can deduce the surface wind turning angle  $\alpha$ , i. e.

$$\alpha \approx \sin^{-1}(5u_*/G) . \quad (6.32)$$

For the case shown, this gives  $\alpha \approx 15^\circ$ , in excellent agreement with the hodograph in Fig. 6.5. Smoother surfaces with lower  $u_*/G$  (e. g. ocean) will give smaller turning angles and rougher surfaces will give larger turning angles, as we'd expect. We can also deduce  $u_g$  ( $\approx 0.96G$  for the case shown). At the top of the surface layer,  $u_s = u_g + u_*F_x(0) \approx u_g - 5u_* \approx (0.96 - 0.27)G = 0.7G$ , again in good agreement with the plotted hodograph once it is rotated into coordinates along/transverse to the surface wind. From this we could deduce a precise matching height  $z_s$  at which  $u_s = (u_*/k) \ln(z_s/z_0)$  between the log-layer and the velocity defect profiles. While this all may seem rather indirect, it provides a way to construct the boundary layer wind and stress profile in any turbulent barotropic Ekman layer. In fact, this would be a wonderful approach to parameterize BLs if they were actually unstratified and barotropic, but this is almost never the case in reality.